Improved load frequency control with chess algorithm-driven optimization of 3DOF-PID controller

Kittipong Ardhan[1], Natpapha Chansom[2], Sitthisak Audomsi[3], Worawat Sa-Ngiamvibool[3,4], Jagraphon Obma[5]

[1]Department of Electrical Engineering, Faculty of Engineering and Industrial Technology, Kalasin University, Kalasin, Thailand
[2]Department of Mechatronics Engineering, Faculty of Engineering, Rajamangala University of Technology ISAN, Khonkaen Campus, Khon Kaen, Thailand
[3]Department of Electrical Engineering, Faculty of Engineering, Mahasarakham University, Maha Sarakham, Thailand
[4]Electrical and Computer Engineering Research Unit, Faculty of Engineering, Mahasarakham University, Maha Sarakham, Thailand
[5]Department of Computer Engineering, Faculty of Engineering, Rajamangala University of Technology ISAN, Khonkaen Campus, Khon Kaen, Thailand

Article Info

ABSTRACT

In contemporary hybrid power systems, persistent load fluctuations disrupt the delicate balance between electrical output and mechanical torque, thereby compromising frequency stability. Load frequency control (LFC) mechanisms are indispensable in maintaining this equilibrium, particularly in systems integrating renewable and thermal energy sources. This study introduces a three-degree-of-freedom proportional-integral-derivative (3DOF-PID) controller optimized via the novel chess optimization algorithm (COA) and evaluates its efficacy against the ant lion optimizer (ALO) and Harris Hawks optimization (HHO). Extensive MATLAB/Simulink simulations were conducted on a hydrothermal system, with performance assessed through objective functions—integral of absolute error (IAE) and integral of time-weighted absolute error (ITAE). The COA consistently yielded the lowest cumulative error values (IAE=0.1548 and ITAE=0.2965), demonstrating its superiority in steady-state performance. However, COA exhibited substantial dynamic deviations, including an overshoot of 387.79% and undershoot of 4513.8% in Δftie. Conversely, HHO offered a significantly enhanced transient response, achieving 0% undershoot in Δftie with minimal oscillatory behavior. ALO displayed moderate performance but struggled with higher undershoots and prolonged settling time. The findings underscore the criticality of algorithm selection in controller design. While COA excels in minimizing long-term errors, HHO is preferable for applications requiring heightened dynamic stability and responsiveness.

Corresponding Author:

Jagraphon Obma
Department of Computer Engineering, Faculty of Engineering
Rajamangala University of Technology ISAN
Khonkaen Campus, Khon Kaen, Thailand
Email: Jagraphon.ob@rmuti.ac.th

1. INTRODUCTION

In an age of swiftly rising energy demands and fluctuating load circumstances, maintaining the stability of contemporary power systems has become paramount [1], [2]. Frequent load fluctuations disrupt the balance between electrical output and mechanical torque in generators, resulting in variations in rotor speed and, subsequently, in system frequency [3], [4]. Load frequency control (LFC) is essential for ensuring

frequency stability and improving system resilience, especially in hybrid energy systems characterized by intrinsic variability [5], [6].

Motivated by environmental issues and technological progress, the amalgamation of renewable energy sources—such as wind, solar, and hydropower—with conventional thermal generating has resulted in the development of hybrid power systems [7]-[9]. These systems, although environmentally beneficial, provide considerable hurdles for frequency regulation due to their unpredictable nature. Ensuring stability in such systems requires extremely adaptable and precise control mechanisms [10]-[13].

Although various optimization techniques, including the ant lion optimizer (ALO) [14] and Harris Hawks optimization (HHO) [15], have been employed for tuning proportional-integral-derivative (PID)-based controllers in LFC applications [16]-[18], they often suffer from limitations such as premature convergence or insufficient handling of nonlinearities in hybrid settings. To address this gap, this study proposes the use of the chess optimization algorithm (COA) to enhance the tuning of a three-degree-of-freedom proportional-integral-derivative (3DOF-PID) controller.

This paper has three primary contributions: i) it presents COA for tuning LFC controllers, ii) it compares COA with ALO and HHO in a hydrothermal setting, and iii) it shows enhanced frequency regulation using MATLAB/Simulink simulations. This research enhances the formulation of more robust and energy-efficient control algorithms for intricate hybrid power systems.

2. MODEL OF THE REHEAT THERMAL AND HYDRO POWER SYSTEMS UNDER INVESTIGATION

The block diagram depicted in Figure 1 represents a two-area hydro-reheat thermal power system that has been examined for load frequency management [19]. A detailed power system can be divided into multiple-LFC areas interconnected by tie-lines. It is possible to investigate a scenario involving two areas connected by a single tie line without any loss of generality [20].
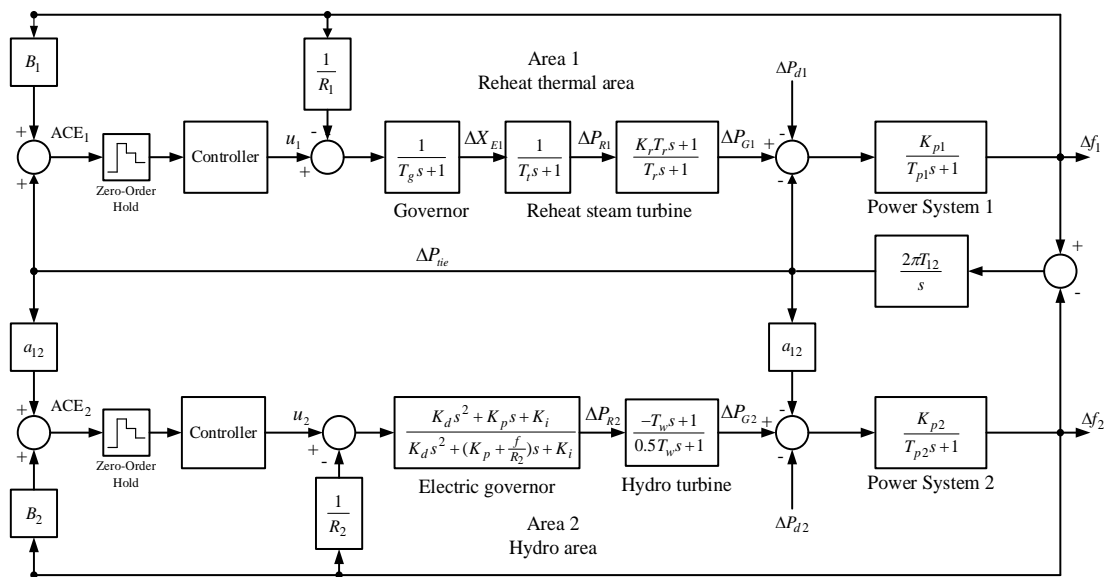

Figure 1. Two area hydro-reheat thermal power system

3. THREE-DEGREE-OF-FREEDOM PROPORTIONAL-INTEGRAL-DERIVATIVE CONTROLLER

Figure 2 presents the block diagram of the 3DOF-PID controller as described in [15]. In this configuration, R(s) refers to the reference input signal, Y(s) corresponds to the tie-line power feedback, and D(s) represents an external disturbance or noise input. The principal objective of the 3DOF-PID controller is to mitigate substantial disturbances while ensuring dynamic responsiveness and robust closed-loop performance. The parameters PW and DW define the set-points for the proportional and derivative paths, respectively [21]. The term N denotes the filter coefficient applied to the derivative path, whereas Gff

accounts for the feedforward gain applied to D(s). The control signal output from the 3DOF-PID, denoted ΔP_c is formulated as (1):

$$\frac{\Delta P_c}{R(s)} = \frac{s^2(K_D NDW + K_P PW) + s(NPW + K_I) + K_I N}{s(s+N)} \tag{1}$$

Where K_P, K_I, and K_D denote the proportional, integral, and derivative gains of the controller, respectively.
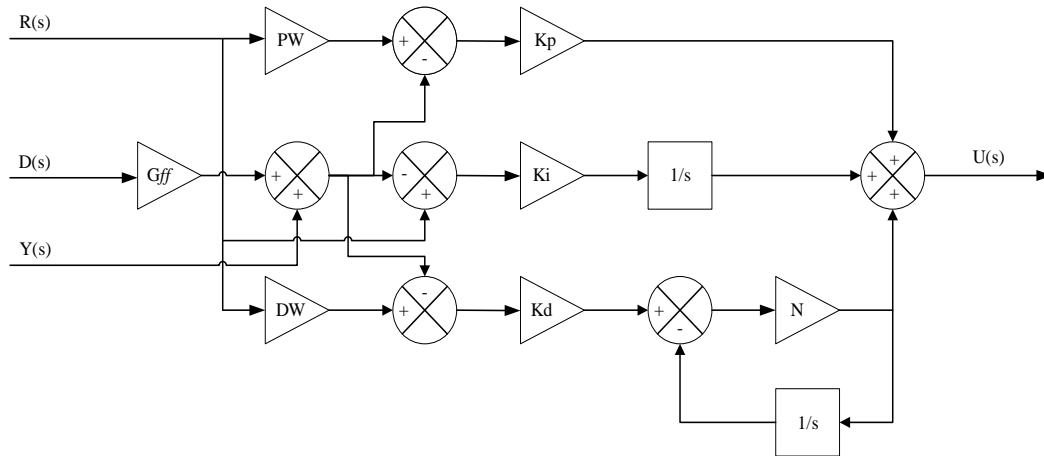

Figure 2. Block diagram of 3DOF-PID controller

4. CHESS OPTIMIZATION ALGORITHM

This study presents an approach called the COA, which utilizes the principles and strategies from the game of international chess to identify the optimal value. Moreover, one must consider the specific movements of each chess piece along with the comprehensive strategic framework of the game. Utilizing the previously mentioned concept to determine the best value will enable the player to secure a win in the game. This will produce an algorithm exhibiting a variety of traits across multiple domains. This concept facilitates the creation of an algorithm, as each chess piece can move in specific ways dictated by a predefined set of rules, reflecting the style of the game. Utilizing these concepts in optimization will lead to the development of algorithms that excel in tackling a wide range of intricate challenges [22]. The Chess algorithm consists of the following steps:

a. Step 1: introduce variability in the solution by allocating 8 pawns (np) in a randomized manner. Responses should be practical and achievable within the given limitations. Given the numerous mandatory requirements, it is essential that the number of iterations remain limited to one.
b. Step 2: assess the random pawn allocations. Each response leads to an evaluation of the function. Being ready to classify the response signifies the function's minimum value.
c. Step 3: display the organized responses. This step includes the sequential arrangement of 1 king, 1 queen, 2 rooks, 2 knights, and 2 bishops.
d. Step 4: allocate items on a one-by-one basis analyze the movements of the pieces to identify the nearby solution.
e. Step 5: assess the responses in the vicinity. Assess the function for each outcome. Identify the most effective options in the vicinity. Every element
f. Step 6: reposition items. Identify the optimal solution for ensuring compatibility between components and their environment.
g. Step 7: analyze the search results in relation to all chess pieces. Which response yields the greatest function value? Identify it as the optimal solution in that search iteration.
h. Step 8: evaluate the conditions and incorporate a local response. Provided that the criteria are fulfilled. Let us liberate ourselves from constrained solutions.
i. Step 9: verify the termination criteria. If the criteria are satisfied, cease further inquiry. Enhance the number of iterations when the requirements remain unfulfilled. Increment the current iteration value by 1 to obtain the updated value.
j. Step 10: evenly distribute 8 pieces and initiate the process again.

k. Step 11: involves combining the current best arrangement for all chess pieces (1 king, 1 queen, 2 rooks, 2 knights, and 2 bishops) with the starting pawn arrangement (8 pieces). This is done while setting the function value of the random pawn selection outcome. The 16 responses were evaluated and ordered from most favorable to least favorable.

l. Step 12: reiterates step 3, focusing on the top 8 responses until the stopping condition is satisfied.

5.   MATHEMATICAL ANALYSIS OF THE PROPOSED SYSTEM

This paper explores the stability of the proposed system through an examination of delay-based factors. The choice of the objective function plays a vital role in improving the dynamic outcomes of the system [23].

5.1. Objective function

In optimal control theory, a cost function is typically associated with attaining the desired control objective through the closed-loop system, whether in the time domain or the frequency domain. Carefully adjusting the controller's free parameters should minimize this function [24].

Integral of absolute error (IAE) serves as a key performance criterion in this study for the optimization assignment. IAE is defined as (2) [25]:

$$IAE = \int_0^{50}(|\Delta f_1|+|\Delta f_2|+|\Delta P_{tie}|)dt \tag{2}$$

Integral of time-weighted absolute error (ITAE) serves as a performance criterion used in this study for the optimization assignment. ITAE is defined as (3) [26]:

$$ITAE = \int_0^{50}(|\Delta f_1|+|\Delta f_2|+|\Delta P_{tie}|) \cdot t \, dt \tag{3}$$

where Δf_i and ΔP_{tie} are the frequency deviation of the power system [27].

5.2. System constraints

The proposed LFC system is characterized as a constrained optimization problem, with the constraints detailed as (4) [28]:

$$K_{Paramiter \, min} \leq K_{Paramiter} \leq K_{Paramiter \, max} \tag{4}$$

The minimum and maximum values of the controller parameters are indicated by the min and max symbols. The lower boundary and the upper boundary for all 14 controllers. The parameters are detailed in Table 1. This investigation utilizes HHO [26], ALO [29], and COA.

Table 1. Minimum and maximum value of the control parameter

Controller parameter	Gain parameter	
	Hydro area	Thermal area
Lower boundary	0	0
Upper boundary	1	1

6.   SIMULATION AND RESULTS

The simulation of the hydro-thermal power system was conducted using MATLAB/Simulink, with a CPU of Core i5-12400F, 16.0 GB DDR4-3200 RAM and an NVIDIA GeForce RTX 4060 GPU. The parameter of the MATLAB simulation is considered as variable-step ODE45-type solvers. The simulation time for each iteration is established at 50 seconds. The m-file contains formulations for the proposed algorithms: HHO, ALO, and COA. The maximum number of iterations is set at 50 for tuning the controller setting in all cases.

6.1. Result using objective function integral of absolute error

The system described is simulated using all four controllers, excluding any communication delay from the analysis. The appendix provides a comprehensive enumeration of the system configuration values for the entire system. The tuning of all controller parameters is conducted through various algorithms,

including ALO, HHO, and COA, as detailed in Table 2. The system's responses regarding the frequency error Δf_i (Figures 3(a) and (b)) and tie-line power error ΔP_{tie} (Figure 3(c)) for various controllers are summarized in Figure 3. The parameters in the time domain for evaluating system performance are presented in Table 2.

Table 2. Parameter setting of the controller using objective function IAE

| Tuned parameters		COA [Proposed]	ALO [Studied]	HHO [Studied]	Tuned parameters		COA [Proposed]	ALO [Studied]	HHO [Studied]
Reheat thermal area	K_p	0.4374	0.0334	1.0000	Hydro area	K_p	0.1318	0.1307	1.0000
	K_i	0.5234	0.4369	0.5724		K_i	0.9414	0.1359	0.0427
	K_d	0.5175	0.4113	0.2868		K_d	0.0466	0.1090	0.0005
	P_w	0.4728	0.0940	1.0000		P_w	0.1138	0.0383	0.0949
	D_w	0.8410	0.7590	0.0006		D_w	0.0212	0.6419	0.1627
	N	0.3333	0.4716	0.1033		N	0.0992	0.0227	0.0003
	G_{ff}	0.0444	0.1552	1.0000		G_{ff}	0.3195	0.1796	0.0001

(a)

(b)

(c)
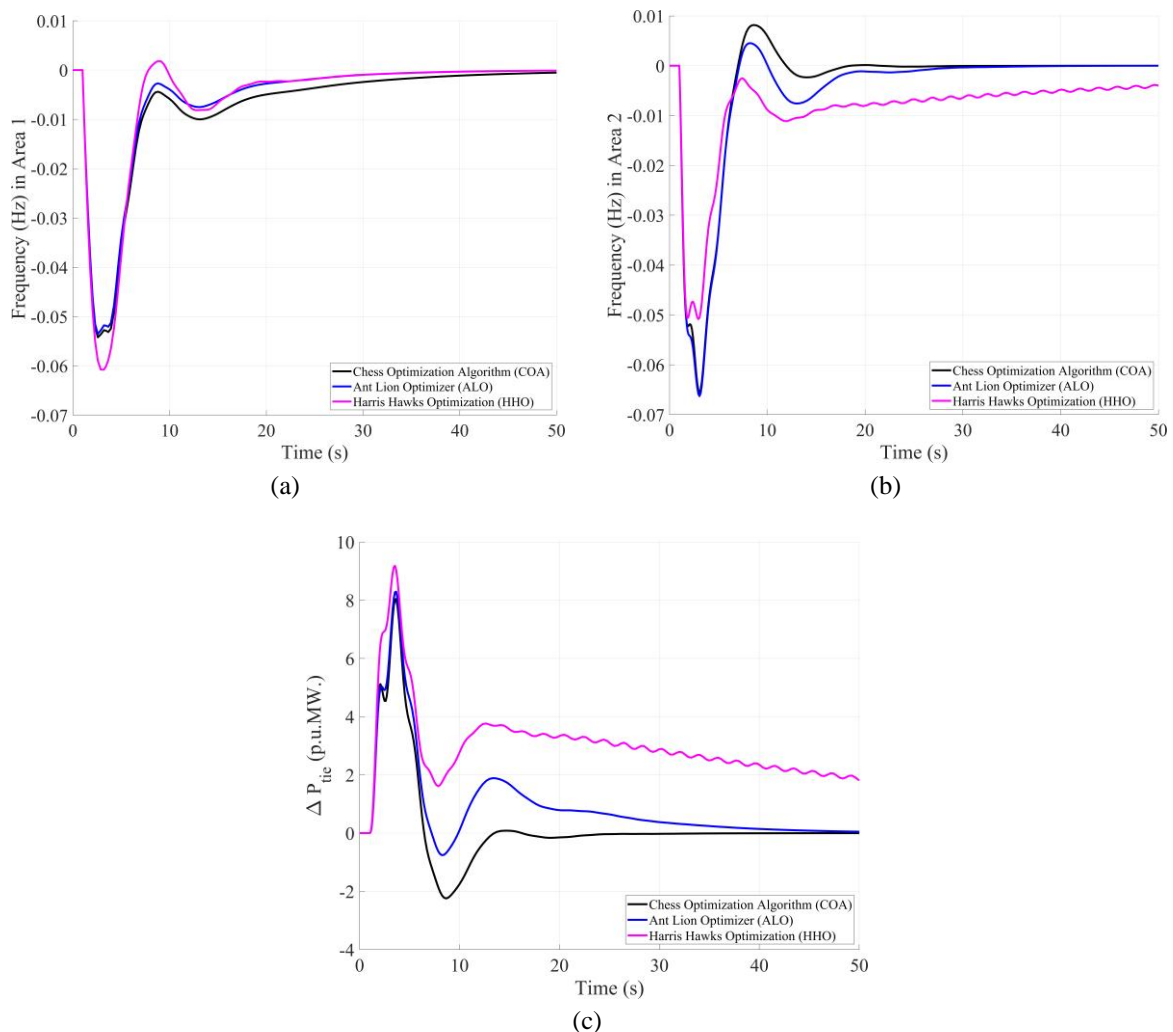
Figure 3. Frequency deviations: (a) reheat thermal zone, (b) hydroelectric zone, and (c) both areas

Figure 3 and Table 3 present an analysis of the time-domain outcomes for the 3DOF-PID controller, which has been tuned using various algorithms. This analysis reveals notable differences in overshoot, undershoot and settling time across the three response functions. The COA exhibits a significant ability to reduce the cumulative error of the system, as evidenced by the minimum (IAE=0.1548). This indicates that COA is very effective in minimizing long-term system errors. However, COA demonstrates significant overshoot, with values such as 8.4210e+03% in Δf_1 and 21.85% in ΔP_{tie}, indicating a considerable degree of oscillation in the system response. In a similar vein, the undershoot values are noteworthy, with figures like

4.6398e+04% in Δf_1 and 8.4304e+03% in ΔP_{tie}, suggesting that the system may not be appropriate for situations that demand quick stability or minimal oscillatory behavior.

Table 3. Time domains outcomes of the system using objective function IAE

| Function | Parameter | 3DOF-PID controller using objective function IAE | | |
		COA [Proposed]	ALO [Studied]	HHO [Studied]
Δf_1	Overshoot	8.42e+03	7.69e+03	902.7076
	Undershoot	4.63e+04	126.4994	113.0894
	Setting time	5.93e+03	5.93e+03	5.92e+03
Δf_2	Overshoot	3.13e+04	1.17e+04	2.28e+03
	Undershoot	1.72e+05	455.6764	336.3630
	Setting time	5.93e+03	5.93e+03	5.91e+03
ΔP_{tie}	Overshoot	21.8549	800.2219	586.9930
	Undershoot	8.43e+03	0	0
	Setting time	5.73e+03	5.86e+03	5.92e+03
	IAE	0.1548	0.1796	0.2682

In comparison, HHO demonstrates the most balanced and stable performance when evaluated against the other algorithms. The results indicate the lowest overshoot values across all response functions, with 902.7076% for Δf_1 (Figure 3(a)) and 586.9930 for ΔP_{tie} (Figure 3(c)). The undershoot values are at their minimum, recorded at 113.0894% for Δf_1 and 336.3630% for Δf_2 (Figure 3(b)). Furthermore, HHO exhibits a reduced settling time relative to COA, with values of 5.9249e+03 seconds for ΔP_{tie} in contrast to 5.7328e+03 seconds for COA.

6.2. Result using objective function integral of time-weighted absolute error

To assess the performance of the 3DOF-PID controller optimized using the COA for LFC, the controller parameters are established in accordance with the ITAE objective function. This approach is designed to ensure a rapid system response while minimizing cumulative error. Table 4 presents the optimized parameter values.

Table 4. Parameter setting of the controller using objective function ITAE

Tuned parameters		COA [Proposed]	ALO [Studied]	HHO [Studied]	Tuned parameters		COA [Proposed]	ALO [Studied]	HHO [Studied]
Reheat thermal area	K_p	0.7830	0.8205	0.0497	Hydro area	K_p	0.1284	0.1484	1.0000
	K_i	0.1157	0.1341	0.2043		K_i	0.0863	0.1358	0.1873
	K_d	0.5887	0.6573	0.4712		K_d	0.0014	0.0010	0.0449
	P_w	0.8936	0.9143	0.1138		P_w	0.0940	0.1172	0.0364
	D_w	0.1425	0.1147	0.0014		D_w	0.1239	0.2014	0.9101
	N	0.8826	0.8609	0.0148		N	0.2685	0.3099	0.0755
	G_{ff}	0.4979	0.5390	0.9262		G_{ff}	0.3324	0.2965	0.6863

The system described earlier is simulated using all four controllers, excluding any communication delay. The appendix provides a comprehensive enumeration of the system configuration values for the entire system. The tuning of all controller parameters is conducted through various algorithms, including the ALO, HHO, and COA, as detailed in Table 5. The system's frequency error responses Δf_i show (Figures 4(a) and (b)) and tie-line power error responses ΔP_{tie} (Figure 4(c)) for various controllers are summarized in Figure 4. The parameters in the time domain for evaluating system performance are presented in Table 5.

The analysis of Table 5, which details the results of the 3DOF-PID system optimized through the COA, ALO, and HHO, clearly indicates that each optimization method has its own unique advantages and limitations. COA shows exceptional performance in reducing the cumulative system error, attaining the lowest ITAE value of 0.2965, in contrast to ALO (0.4932) and HHO (1.0622). Nonetheless, COA continues to demonstrate a higher Overshoot in certain functions, such as ΔP_{tie} at 387.7896%, surpassing that of ALO (205.9978%). Furthermore, the COA's undershoot Δf_1 is recorded at 1.3696e+03%, which, while lower than ALO's 4.8165e+04%, is still considerably higher than HHO's 59.3990%.

Table 5. Time domains the outcomes of the system using objective function ITAE

Function	Parameter	COA [Proposed]	ALO [Studied]	HHO [Studied]
		3DOF-PID controller using objective function ITAE		
Δf_1	Overshoot	131.5172	3.71e+05	1.76e+03
	Undershoot	1.36e+03	4.81e+04	59.3990
	Setting time	5.93e+03	5.94e+03	5.79e+03
Δf_2	Overshoot	2.23e+03	3.06e+03	2.38e+03
	Undershoot	420.4494	1.70e+04	207.9822
	Setting time	5.93e+03	5.93e+03	5.82e+03
ΔP_{tie}	Overshoot	387.7896	205.9978	449.1254
	Undershoot	4.51e+03	8.04e+03	0
	Setting time	5.93e+03	5.93e+03	5.83e+03
	ITAE	0.2965	0.4932	1.0622
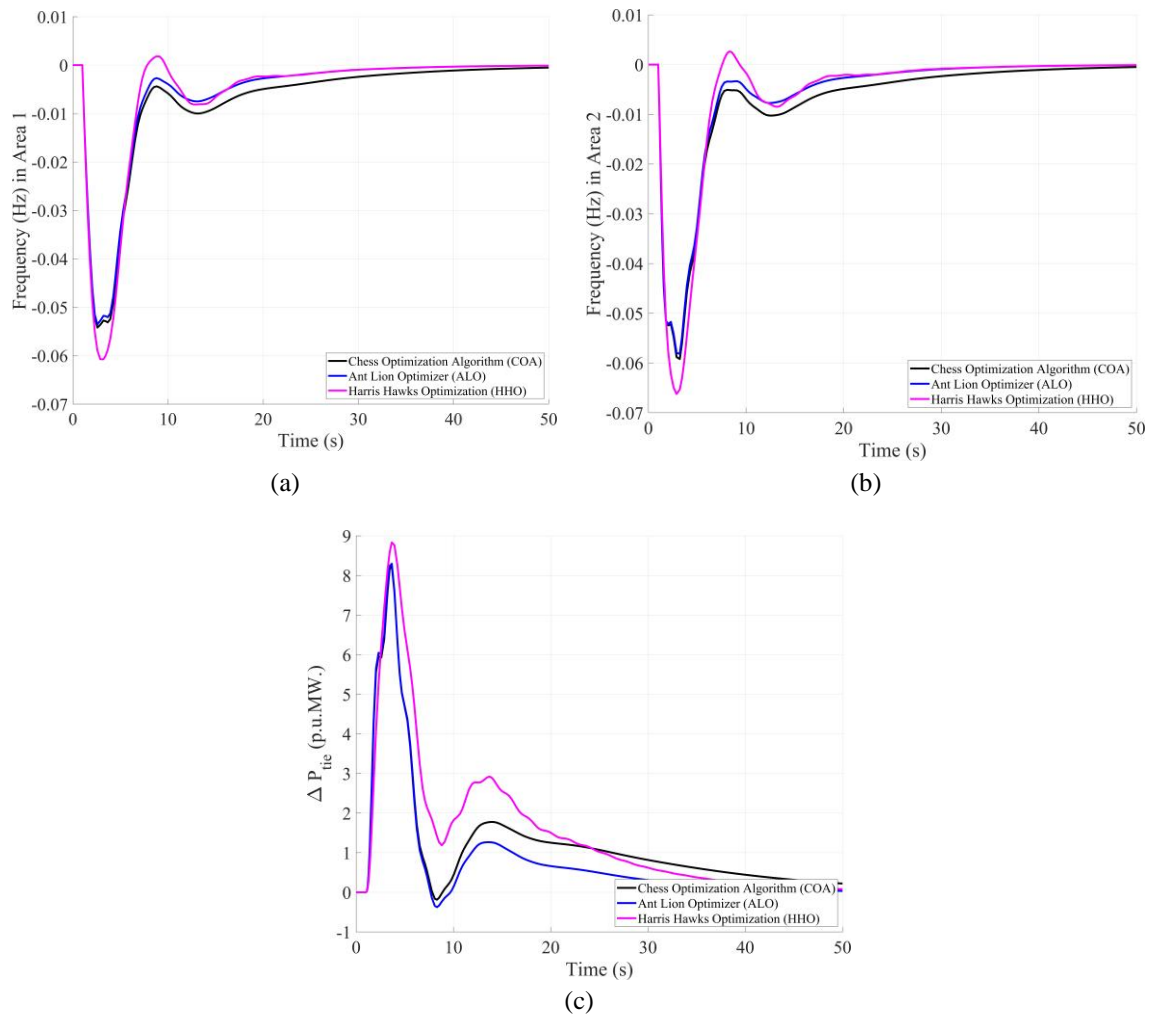
Figure 4. Frequency deviations: (a) reheat thermal zone, (b) hydroelectric zone, and (c) both areas

Conversely, HHO exhibits exceptional stability in the system's response, showcasing the lowest Overshoot values in multiple instances, including Δf_1 at 1.7640e+03%, in contrast to COA (131.5172%) and ALO (3.7130e+05%). Moreover, HHO greatly reduces undershoot, as demonstrated in ΔP_{tie}, achieving 0% and surpassing COA (4.5138e+03%) and ALO (8.0474e+03%). The settling time for HHO demonstrates a competitive edge, as indicated by ΔP_{tie}, achieving 5.8337e+03 seconds, which is marginally lower than COA at 5.9395e+03 seconds and closely aligns with ALO at 5.9363e+03 seconds.

7. CONCLUSION

This study employed the COA, ALO, and HHO to tune the parameters of a 3DOF-PID controller for LFC in a hydrothermal power system. Simulation results reveal that COA demonstrates outstanding long-term error minimization, achieving the lowest IAE and ITAE (0.2965), while HHO offers superior dynamic response with minimal overshoot and undershoot—undershoot of 0% in ΔP_{tie}—making it ideal for stability-sensitive applications. ALO provides moderate performance, showing improved overshoot in some cases but struggling with settling time and undershoot.

The findings underscore the importance of aligning the choice of optimization algorithm with specific control objectives: COA is well-suited for minimizing cumulative errors, whereas HHO is preferable in scenarios requiring enhanced transient stability and rapid convergence. In terms of real-world applications, COA-tuned 3DOF-PID controllers hold promises for deployment in advanced power grids, particularly hybrid systems integrating renewable and thermal sources, where precise frequency regulation is critical.

Nonetheless, this study is limited to simulation-based validation in a hydrothermal context. Future research should explore real-time implementation in large-scale power networks, investigate hybrid approaches that integrate COA with deep learning techniques, and assess controller robustness under varying levels of renewable energy penetration.

FUNDING INFORMATION

AUTHOR CONTRIBUTIONS STATEMENT

This journal uses the Contributor Roles Taxonomy (CRediT) to recognize individual author contributions, reduce authorship disputes, and facilitate collaboration.

Name of Author	C	M	So	Va	Fo	I	R	D	O	E	Vi	Su	P	Fu
Kittipong Ardhah	✓			✓	✓	✓	✓	✓	✓				✓	✓
Natpapha Chansom		✓		✓	✓					✓				
Sitthisak Audomsi	✓	✓	✓	✓	✓	✓	✓	✓	✓	✓	✓			
Worawat Sa-Ngiamvibool	✓		✓	✓		✓	✓			✓		✓		
Jagraphon Obma	✓	✓		✓	✓	✓	✓	✓	✓	✓	✓	✓	✓	✓

C : **C**onceptualization	I : **I**nvestigation	Vi : **Vi**sualization
M : **M**ethodology	R : **R**esources	Su : **Su**pervision
So : **So**ftware	D : **D**ata Curation	P : **P**roject administration
Va : **Va**lidation	O : Writing - **O**riginal Draft	Fu : **Fu**nding acquisition
Fo : **Fo**rmal analysis	E : Writing - Review & **E**diting	

CONFLICT OF INTEREST STATEMENT

The authors declare no conflict of interest.

DATA AVAILABILITY

There is no data which used for this study.

REFERENCES

[1] J. Sousa, A. Sousa, F. Brueckner, L. P. Reis, and A. Reis, "Human-in-the-loop Multi-objective Bayesian Optimization for Directed Energy Deposition with in-situ monitoring," *Robotics and Computer-Integrated Manufacturing,* vol. 92, 2025, doi: 10.1016/j.rcim.2024.102892.
[2] Y. Han, Z. Dong, C. Cui, T. Zhang, and Y. Luo, "Multi-objective optimization scheduling for extensive plain lake water resources incorporating flood resource utilization," *Journal of Hydrology,* vol. 651, 2025, doi: 10.1016/j.jhydrol.2024.132584.
[3] B. Xie *et al.*, "Advances in Graphene-Based Electrode for Triboelectric Nanogenerator," *Nano-Micro Letters,* vol. 17, no. 1, 2025, doi: 10.1007/s40820-024-01530-1.
[4] Y. Liu, J. Liu, K. Xue, and J. Seok, "Development of a novel wake-induced rotational galloping wind energy harvester and the identification of its working mechanism," *Mechanical Systems and Signal Processing,* vol. 224, 2025, doi: 10.1016/j.ymssp.2024.112019.

[5]   S. Cuoghi, L. K. Pittala, R. Mandrioli, V. Cirimele, M. Ricco, and G. Grandi, "Model-based adaptive control of modular DAB converter for EV chargers," *IET Power Electronics,* vol. 17, no. 16, pp. 2669-2685, 2024, doi: 10.1049/pel2.12709.

[6]   H. Benlaria, "Does Education Spending Affect Energy Consumption in Saudi Arabia? A Bootstrap Causality Test," *International Journal of Energy Economics and Policy,* vol. 15, no. 1, pp. 36-46, 2025, doi: 10.32479/ijeep.17481.

[7]   M. S. Mauludin, M. Khairudin, R. Asnawi, W. A. Mustafa, and T. S. Fauziah, "The Advancement of Artificial Intelligence's Application in Hybrid Solar and Wind Power Plant Optimization: A Study of the Literature," *Journal of Advanced Research in Applied Sciences and Engineering Technology,* vol. 50, no. 2, pp. 279-293, 2025, doi: 10.37934/araset.50.2.279293.

[8]   V. Kumar, S. Sharma, S. Sharma, and A. Dev, "Optimal voltage and frequency control strategy for renewable-dominated deregulated power network," *Scientific Reports,* vol. 15, no. 1, 2025, doi: 10.1038/s41598-024-84549-z.

[9]   Y. Li, F. Kong, C. Jing, and L. Yang, "MILP model for peak shaving in hydro-wind-solar-storage systems with uncertainty and unit commitment," *Electric Power Systems Research,* vol. 241, 2025, doi: 10.1016/j.epsr.2024.111358.

[10] A. Villamarín-Jácome, M. Saltos-Rodríguez, D. Espín-Sarzosa, R. Haro, G. Villamarín, and M. O. Okoye, "Deploying renewable energy sources and energy storage systems for achieving low-carbon emissions targets in hydro-dominated power systems: A case study of Ecuador," *Renewable Energy,* vol. 241, 2025, doi: 10.1016/j.renene.2024.122198.

[11] A. Merabet, A. Al-Durra, T. El-Fouly, and E. F. El-Saadany, "Optimization and energy management for cluster of interconnected microgrids with intermittent non-polluting and diesel generators in off-grid communities," *Electric Power Systems Research,* vol. 241, 2025, doi: 10.1016/j.epsr.2024.111319.

[12] D. Tripathy, B. K. Sahu, B. Patnaik, and N. B. D. Choudhury, "Spider monkey optimization based fuzzy-2D-PID controller for load frequency control in two-area multi source interconnected power system," in *International Conference on Technologies for Smart City Energy Security and Power: Smart Solutions for Smart Cities, ICSESP 2018 - Proceedings*, 2018, pp. 1-6, doi: 10.1109/ICSESP.2018.8376743.

[13] P. Sreenivasan, L. Dhandapani, S. Natarajan, A. D. Adaikalam, and A. Sivakumar, "Improved load frequency control in dual-area hybrid renewable power systems utilizing PID controllers optimized by the salp swarm algorithm," *International Journal of Power Electronics and Drive Systems,* vol. 15, no. 3, pp. 1711-1718, 2024, doi: 10.11591/ijpeds.v15.i3.pp1711-1718.

[14] I. F. Davoudkhani, P. Zare, A. Y. Abdelaziz, M. Bajaj, and M. B. Tuka, "Robust load-frequency control of islanded urban microgrid using 1PD-3DOF-PID controller including mobile EV energy storage," *Scientific Reports,* vol. 14, no. 1, 2024, doi: 10.1038/s41598-024-64794-y.

[15] S. Chakraborty, A. Mondal, and S. Biswas, "Application of FUZZY-3DOF-PID controller for controlling FOPTD type communication delay based renewable three-area deregulated hybrid power system," *Evolutionary Intelligence,* vol. 17, no. 4, pp. 2821-2841, 2024, doi: 10.1007/s12065-024-00914-x.

[16] M. Gengaraj, L. Kalaivani, and R. Rajesh, "Investigation on Torque Sharing Function for Torque Ripple Minimization of Switched Reluctance Motor: A Flower Pollination Algorithm Based Approach," *IETE Journal of Research,* vol. 69, no. 6, pp. 3678-3692, 2023/08/18 2023, doi: 10.1080/03772063.2022.2112312.

[17] M. P. E. Rajamani, R. Rajesh, and M. W. Iruthayarajan, "A PID control scheme with enhanced non-dominated sorting genetic algorithm applied to a non-inverting buck-boost converter," *Sādhanā,* vol. 47, no. 4, p. 222, 2022, doi: 10.1007/s12046-022-02012-z.

[18] R. Rajesh, P. V. Gaurkar, G. Vivekanandan, S. Sivaram, and S. C. Subramanian, "Impact of wheel speed signal processing on Antilock Brake System in heavy road vehicles," *Vehicle System Dynamics,* pp. 1-22, 2023, doi: 10.1080/00423114.2025.2476745.

[19] C. Jan-Ngurn *et al.*, "Development of PV/Battery Grid-Connected System for Efficient Charging of Plug-in Electric Vehicles in Residential Areas in Thailand," *Engineering Access,* vol. 11, no. 2, pp. 293-300, 2025, doi: 10.14456/mijet.2025.30.

[20] R. Rajesh and S. N. Deepa, "Design of direct MRAC augmented with 2 DoF PIDD controller: An application to speed control of a servo plant," *Journal of King Saud University - Engineering Sciences,* vol. 32, no. 5, pp. 310-320, 2020, doi: 10.1016/j.jksues.2019.02.005.

[21] R. Rajesh, "Optimal tuning of FOPID controller based on PSO algorithm with reference model for a single conical tank system," *SN Applied Sciences,* vol. 1, no. 7, p. 758, 2019, doi: 10.1007/s42452-019-0754-3.

[22] P. Nuamkoksung *et al.*, "Integrated Control of DER Placement and Network Reconfiguration in EV-Charging Distribution Systems Using Multi-Optimization Techniques," *Engineering Access,* vol. 11, no. 2, pp. 301-318, 2025, doi: 10.14456/mijet.2025.31.

[23] M. P. E. Rajamani, R. Rajesh, and M. W. Iruthayarajan, "Design and Experimental Validation of PID Controller for Buck Converter: A Multi-Objective Evolutionary Algorithms Based Approach," *IETE Journal of Research,* vol. 69, no. 1, pp. 21-32, 2023, doi: 10.1080/03772063.2021.1905564.

[24] A. Moloody, A. As'arry, T. S. Hong, R. Kamil, and A. Zolfagharian, "PID Controller Parameter Tuning Based on a Modified Differential Evolutionary Optimization Algorithm for the Intelligent Active Vibration Control of a Combined Single Link Robotics Flexible Manipulator," *Journal of Advanced Research in Applied Sciences and Engineering Technology,* vol. 52, no. 1, pp. 234-258, 2025, doi: 10.37934/araset.52.1.234258.

[25] A. P. A. Neto, W. M. M. Santos, and R. P. Brito, "Intelligent control system applied to the recovery of tetrahydrofuran and ethyl acetate from Waste Effluent by using indirect-extractive distillation," *Separation and Purification Technology,* vol. 358, 2025, doi: 10.1016/j.seppur.2024.130446.

[26] S. Shirali, S. Z. Moghaddam, and M. Aliasghary, "An interval Type-2 fuzzy Fractional-Order PD-PI controller for frequency stabilization of islanded microgrids optimized with CO algorithm," *International Journal of Electrical Power and Energy Systems,* vol. 164, 2025, doi: 10.1016/j.ijepes.2024.110422.

[27] R. Ramakrishnan and D. S. Nachimuthu, "Design of State Feedback LQR Based Dual Mode Fractional-Order PID Controller using Inertia Weighted PSO Algorithm: For Control of an Underactuated System," *Journal of The Institution of Engineers (India): Series C,* vol. 102, no. 6, pp. 1403-1417, 2021, doi: 10.1007/s40032-021-00756-x.

[28] Z. Chen *et al.*, "A two-stage hybrid model for dissolved oxygen prediction and control in aquaculture," *Aquaculture International,* vol. 33, no. 1, 2025, doi: 10.1007/s10499-024-01791-y.

[29] J. A. Guzmán-Henao, R. I. Bolaños, B. Cortés-Caicedo, L. F. Grisales-Noreña, O. D. Montoya, and J. C. Hernández, "A multi-objective master–slave methodology for optimally integrating and operating photovoltaic generators in urban and rural electrical networks," *Results in Engineering,* vol. 24, 2024, doi: 10.1016/j.rineng.2024.103059.

BIOGRAPHIES OF AUTHORS

Kittipong Ardhan obtained a B.Eng. in Electrical Engineering from King Mongkut's University of Technology Thonburi (KMUTT), followed by an M.Eng. and Ph.D. in Electrical and Computer Engineering from Maha Sarakham University (MSU), Thailand. His research interests encompass interdigital capacitors and power systems. Since 2023, he has been affiliated with the Faculty of Engineering and Industrial Technology at Kalasin University (KSU), Thailand, where he presently serves as a lecturer in Electrical Engineering. He can be contacted at email: Kittipong.ar@ksu.ac.th.

Natpapha Chansom obtained a B.Sc. degree in computer technology from Rajamangala University of Technology Thanvaburi, followed by an M.Eng. and Ph.D. in electrical and computer engineering from Maha Sarakham University (MSU), Thailand. Her research interests encompass two-sided interdigital capacitor sensors. Since 2023, she has been affiliated with the Department of Mechatronics Engineering at Rajamangala University of Technology ISAN, Khonkaen Campus, Thailand, where she presently serves as a lecturer in electrical engineering. She can be contacted at email: natpapha.ch@rmuti.ac.th.

Sitthisak Audomsi received his present undertaking of a Ph.D. at the Department of Electrical and Computer Engineering. He earned a master's degree in electrical and computer engineering in 2024 and a bachelor's degree in electrical engineering in 2023. The Faculty of Engineering at Mahasarakham University emphasizes research on control systems, optimization techniques, and artificial intelligence. He can be contacted at email: Sitthisak.seagame@gmail.com.

Worawat Sa-Ngiamvibool received his B.Eng. degree in Electrical Engineering, the M.Eng. degree in Electrical Engineering from the Khonkaen University (KKU), Thailand and the Ph.D. degree in Engineering from Sirindhorn International Institute of Technology (SIIT), Thammasat University, Thailand. His research interests include analog circuits and power systems. Since 2007, he has been with Faculty of Engineering, Mahasarakham University (MSU), Thailand, where he is currently a Professor of Electrical Engineering. He can be contacted at email: wor.nui@gmail.com.

Jagraphon Obma obtained his B.Eng. in Electronic and Telecommunication Engineering from Rajamangala University of Technology ISAN, Khonkaen Campus, followed by his M.Eng. and Ph.D. in Electrical and Computer Engineering from Mahasarakham University (MSU), Thailand. His research interests include interdigital capacitor sensors and applications in embedded systems. Since 2015, he has been affiliated with the Department of Computer Engineering at Rajamangala University of Technology ISAN, Khonkaen Campus, where he currently serves as a lecturer in computer engineering. He can be contacted at email: Jagraphon.ob@rmuti.ac.th.